Modeling of a capacitively coupled radio-frequency methane plasma: Comparison between a one-dimensional and a two-dimensional fluid model

D. Herrebout, A. Bogaerts,[a)] M. Yan, and R. Gijbels
Department of Chemistry, University of Antwerp, Universiteitsplein 1, 2610 Wilrijk, Belgium

W. Goedheer
FOM-Institute for Plasma Physics Rijnhuizen, P.O. Box 1207, 3430 BE Nieuwegein, The Netherlands

A. Vanhulsel
Vlaamse Instelling voor Technologisch Onderzoek (VITO), Boeretang 200, 2400 Mol, Belgium

(Received 26 March 2002; accepted for publication 25 June 2002)

A comparison is made between a one-dimensional (1D) and a two-dimensional (2D) self-consistent fluid model for a methane rf plasma, used for the deposition of diamond-like carbon layers. Both fluid models consider the same species (i.e., 20 in total; neutrals, radicals, ions, and electrons) and the same electron–neutral, ion–neutral, and neutral–neutral reactions. The reaction rate coefficients of the different electron–neutral reactions depend strongly on the average electron energy, and are obtained from the simplified Boltzmann equation. All simulations are limited to the alpha regime, hence secondary electrons are not taken into account. Whereas the 1D fluid model considers only the distance between the electrodes (axial direction), the 2D fluid model takes into account the axial as well as the radial directions (i.e., distance between the electrodes and the radius of the plasma reactor, respectively). The calculation results (species densities and species fluxes towards the electrodes) obtained with the 1D and 2D fluid model are in relatively good agreement. However, the 2D fluid model can give additional information on the fluxes towards the electrodes, as a function of electrode radius. It is found that the fluxes of the plasma species towards both electrodes show a nonuniform profile, as a function of electrode radius. This will have an effect on the uniformity of the deposited layer. [DOI: 10.1063/1.1500789]

I. INTRODUCTION

Diamond-like carbon layers are frequently deposited on a variety of materials using plasma-assisted chemical vapor deposition (PACVD). These diamond-like carbon layers (also called amorphous hydrogenated carbon layer, a-C:H), are applied, among others, as wear resistant and low friction coatings. In this article, the simulation of a capacitively coupled rf methane plasma will be discussed using a 1D and a 2D fluid model. In recent years, a number of 1D fluid models have been described[1–3] for the simulation of capacitively coupled rf methane plasmas. The models differ from each other in the way they treat the electron dynamics, and the number of species and reactions taken into account. The input for the fluid model (i.e., reaction rate coefficients, electron and ion mobility and diffusion coefficients) used in Refs. 1 and 2 is obtained from a commercial Boltzmann solver, and is compared with swarm data. From these data, a correlation is obtained between the average electron energy and the ratio E/p (where E represents the dc electric field value and p the pressure). The 1D fluid model described in Ref. 3 makes use of the electron energy distribution function (EEDF), obtained from a similar Boltzmann model. In this way, the electron reaction rate coefficients are calculated as a function of average electron energy. Although the electric field used in the Boltzmann solver differs from the actual field in the discharge, this method gives a good approximation of the EEDF (from which the reaction rate coefficients for the different electron–neutral reactions are calculated), as shown by Meijer *et al.*[4]

This simplified Boltzmann method is also used in combination with the 2D fluid model for methane, which will be discussed in this article. The combination of a fluid model (1D and 2D) with a Boltzmann solver for the calculation of the EEDF, was originally used for silane plasmas.[5–7] Information can be found about a 2D fluid model for a methane plasma, developed by Bera *et al.*,[2,8–10] using swarm data as input. Finally, the use of a particle-in-cell/Monte Carlo (PIC/MC) model, for the simulation of methane plasmas, is reported in Ref. 11. Although a PIC/MC model is the most accurate approach, because it considers the plasma species on the lowest microscopic level, it is very time consuming: hence, a limited number of species can be considered within a reasonable time scale compared to the fluid model.

II. DESCRIPTION OF THE FLUID MODEL

A. 1D fluid model

The 1D fluid model is based on the first three moments of the Boltzmann equation.[12,13] For every species (electrons, ions, neutrals, and radicals), a mass balance equation is considered. The fluxes of the different species are calculated with transport equations by means of the drift-diffusion approximation. Furthermore, the electron energy equation is

[a)]Electronic mail: bogaerts@uia.ua.ac.be

TABLE I. Different species taken into account in the methane plasma model.

Neutrals		Ions			Radicals		Electrons
CH_4	H_2	CH_4^+	CH_3^+	H_2^+	C_2H_5	CH_3	e
C_2H_6	C_3H_8	CH_5^+	$C_2H_5^+$	H_3^+	CH_2	CH	
C_2H_4	C_2H_2	$C_2H_4^+$	$C_2H_2^+$		H		

taken into account. No ion energy equation is considered because it is assumed that the ion energy is equal to the neutral gas thermal energy. The electric field is calculated using the Poisson equation. Because the ions cannot follow the actual electric field, an effective field is used. In order to take into account the influence of the mass flow, some additional terms are incorporated in the mass balance equations of the neutrals. In this way, a simplified gas flow model is incorporated in the 1D fluid model (see Refs. 5–7 for a detailed description). A Sharfetter Gummel scheme is used for the spatial discretisation of the transport equations.[5–7,13–15] In order to solve these equations, a fully implicit method is used. The rf cycle (13.56 MHz) is divided in 80 time steps (i.e., 9.2×10^{-10} s). The neutral–neutral chemistry is calculated, with the time step for the neutrals set to 10^{-6} s.

The distance between the electrode plates of the capacitively coupled rf plasma is set to 2.7 cm. One electrode is grounded, while the other electrode is connected to a power supply, with a rf frequency (ν_{rf}) of 13.56 MHz. The potential of the powered electrode is set to

$$V_t = V_{rf}\sin(2\pi\nu_{rf}t)$$

with V_{rf} the amplitude of the potential. In the model, this value is adapted gradually until the dissipated power (i.e., the power given to the charged species by ohmic heating) equals the electric power, which is an input parameter in the fluid model. The 1D fluid model is applied here for methane and is described in detail in Ref. 3. It takes into account 20 species as illustrated in Table I. The main neutral molecules are CH_4 and H_2. Furthermore, the higher hydrocarbon molecules (i.e., C_2H_6, C_3H_8, C_2H_2, and C_2H_4) are also considered. The main ions are CH_5^+, $C_2H_5^+$, and CH_4^+. The most important radicals included in the model are CH_3, H, and C_2H_5. The reactions considered in the model are: 27 electron–neutral reactions, seven ion–neutral reactions, and 12 neutral–neutral reactions.[3] While the reaction rate coefficients of the ion–neutral and neutral–neutral reactions are taken from the literature, the rate coefficients of the electron–neutral reactions are obtained from the simplified Boltzmann model, as a function of average electron energy. In the Boltzmann model, the EEDF is calculated for a large number of electric field values. From these distribution functions, both the average electron energy, and the reaction rate coefficients for the different electron reactions are calculated. In this way, a table [reaction rate coefficient versus average electron energy (0–20 eV)] is obtained for every electron reaction. The convergence criterion of the fluid model is defined as the error between the discharge parameters (density of the species, potential, electron energy, electron density) at the beginning of two subsequent rf periods, and is set to 10^{-6}. This value was chosen after it was found that a comparison of the results of some simulations with a value set to 10^{-6} and 10^{-7} showed no large differences. A deposition model, based on sticking coefficients,[3] is also included. Although a 1D fluid model is a very useful tool to investigate the plasma chemistry, its disadvantage is that obviously no information can be obtained about the fluxes as a function of the electrode radius. Finally, it should be mentioned that for the conditions under study here, the rf discharge operates in the alpha regime, hence secondary electrons could be neglected.

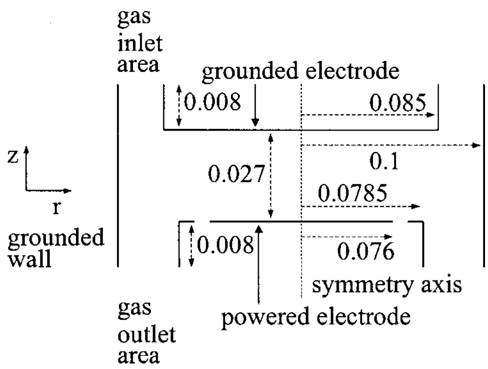

FIG. 1. Schematic diagram of the cylindrically symmetric plasma reactor (with H geometry) used for the 2D calculations. The various dimensions are indicated in meters.

B. 2D fluid model

The 2D fluid model is similar to the 1D model (see Sec. II A) as far as species and reactions are concerned, but is it extended to the radial direction. In this way, information is obtained about plasma characteristics (species densities, potential, etc.) in the z and r position (i.e., the distance between the electrodes and the radius of the plasma reactor, respectively). A scheme of the reactor geometry is given in Fig. 1. This kind of reactor is often used for the deposition of thin layers on materials.[5,6] The distance between the electrodes is 2.7 cm, as in the 1D model, whereas the total radius of the plasma reactor is 10 cm. The geometry is a so-called (cylindrically symmetrical) H geometry. On the upper side, the grounded electrode (with a radius of 8.5 cm) is located next to the inlet region. On the lower side, the rf powered electrode (with a radius of 7.6 cm) is situated next to the outlet region. Except for the rf electrode, all other surfaces are grounded.

In order to avoid numerical instabilities, the grid should contain enough grid points in z and r position. The distance between the electrodes (2.7 cm) is divided into 96 grid points, while the r position (10 cm) contains 72 grid points. The z directions of the inlet and outlet region are further divided into 32 grid points.

The transport of the neutrals is assumed to be governed only by diffusion, therefore, no convective flow is taken into account. This seems justified when the distance between the electrodes is small enough (i.e., only a few centimeters),[6,7] and when the gas inlet flow is rather small (i.e., 20 sccm in our case). In the model, the applied voltage is prescribed as:

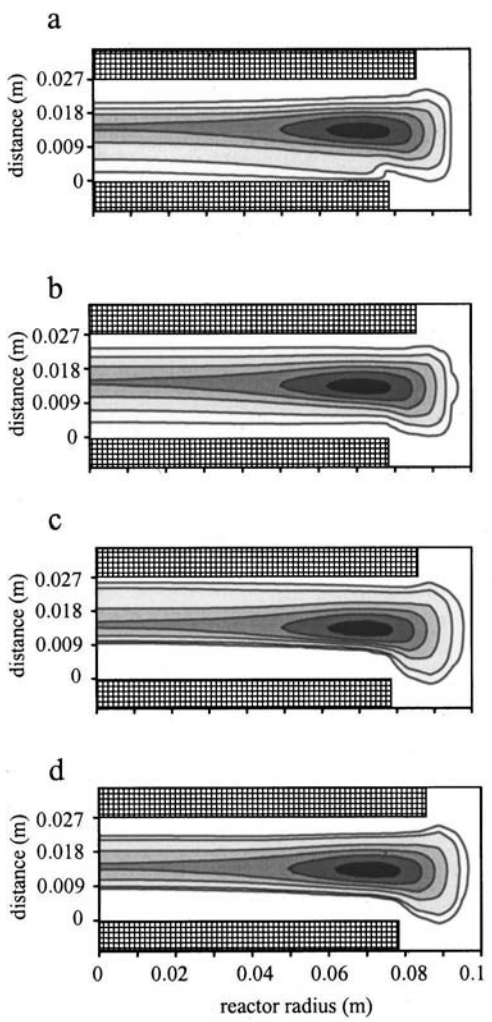

FIG. 2. Calculated 2D electron density profiles (m^{-3}) at the four different phases in the rf cycle, at a power of 5 W: [(a) phase $\pi/2$; (b) phase π; (c) phase $3\pi/2$; (d) phase 2π].

$$V_t = V_{rf} \sin(2\pi \nu_{rf} t) + V_{dc},$$

where V_{rf} is adapted to meet the preset power, in a similar way as in the 1D model. Averaged over one rf cycle, the total electron and ion flux towards both electrodes must be equal. In order to obtain this condition at the powered electrode, the V_{dc} bias voltage is implemented. The value of V_{dc} is gradually adapted in the code, until the fluxes of the electrons and ions to the rf electrode, averaged over one rf cycle, are equal. The disadvantage of the 2D fluid model is however, that these simulations are very computer intensive (i.e., the 2D fluid model can be regarded as a large number of 1D fluid models which have to be solved, in order to take into account the radial and axial direction). While the 1D simulation takes approximately half a day computer time on a professional workstation (alpha processor: EV67), the 2D fluid model requires nearly one week computer time.

III. COMPARISON OF THE RESULTS OF THE 1D AND 2D FLUID MODELS

Simulations have been carried out with both fluid models at four different power values: 5, 10, 15, and 20 W, whereas the other plasma parameters are kept constant. The rf frequency is set to 13.56 MHz, the pressure is set to 0.225 Torr, the inlet gas flow is set to 20 sccm CH_4, and no H_2 is pumped in. For the two fluid models, the distance between the electrodes is set to 2.7 cm.

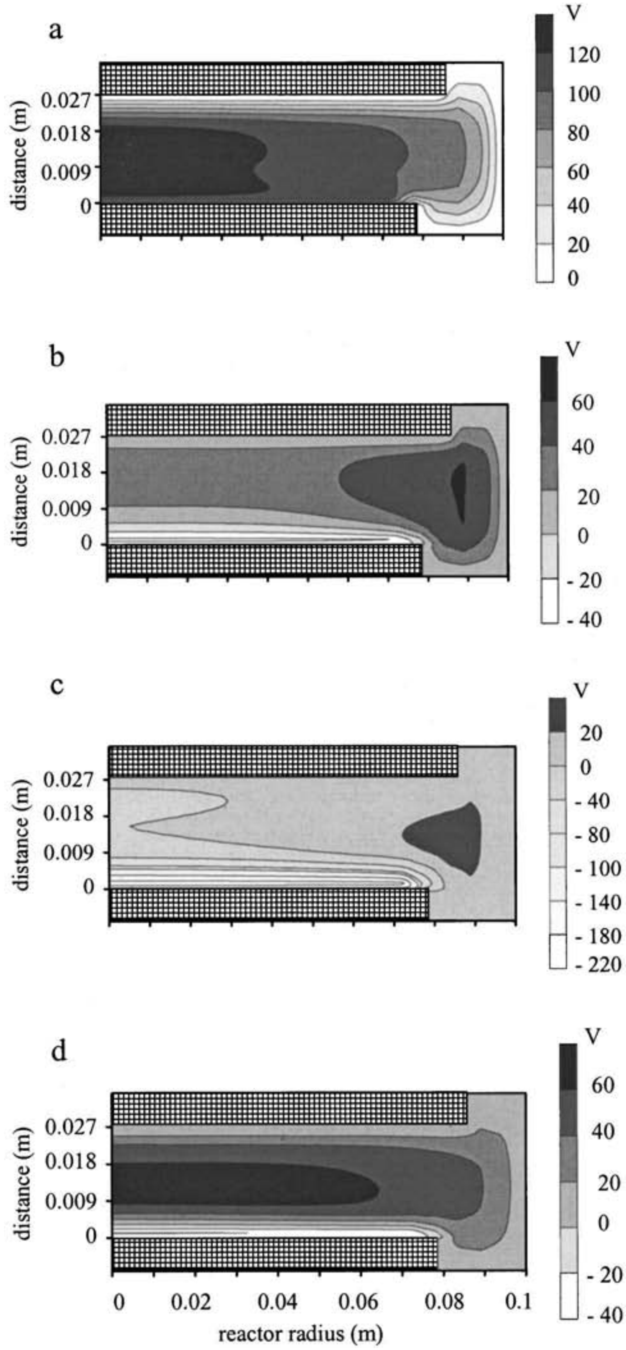

FIG. 3. Calculated 2D potential profiles at the four different phases in the rf cycle, at a power of 5 W; [(a) phase $\pi/2$; (b) phase π; (c) phase $3\pi/2$; (d) phase 2π].

For the 1D fluid model for methane,[3] an extensive comparison was already made between the calculated and experimental species densities available in the literature. In the 1D model, the densities of the charged species and the radicals reach a maximum in the center of the plasma. With the 2D fluid model, information is also obtained on the species densities as a function of radial direction. Figure 2 shows the

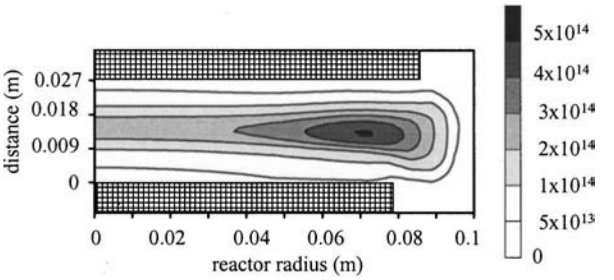

FIG. 4. Calculated 2D time-averaged ion density profile of CH_5^+ (m^{-3}), at a power of 5 W.

electron density at four phases ($\pi/2$, π, $3\pi/2$, 2π) in the rf cycle, calculated with the 2D fluid model, at a power of 5 W. As shown in this figure, the electron density (at the four phases in the rf cycle) is at maximum (nearly 10^{15} m^{-3}) at a radial distance of about 7 cm, which corresponds more or less to the maximum radius of the powered electrode. In Fig. 3, the potential distribution is given at four phases of the rf cycle. From the potential, the electric field can be calculated ($E = -\nabla V$). Due to the larger potential differences at the end of the powered electrode (compared to the region near the axis), the electric field is larger in this region (during part of the rf cycle). Hence in this region, electrons will obtain more energy. This leads to more electron–neutral reactions (i.e., also ionization reactions from which electrons are created) in this region, resulting in a higher electron density (1×10^{15} m^{-3}), compared to the region near the axis (5×10^{14} m^{-3}). Similar 2D electron density profiles are also found in Refs. 8 and 9 for conditions comparable with our input parameters (power, frequency, pressure). From Fig. 2, a change in electron density can also be noticed in the sheath zones of both electrodes, during the rf cycle. Figure 4 shows the calculated time-averaged 2D ion density profile of the main ion species, i.e., CH_5^+ (5 W). It is clear that the ion density is also at its maximum (5×10^{14} m^{-3}) at the edge of the electrode (i.e., radius of 7 cm), similar to the electron density profile. This high ion density can be explained from the more frequent electron reactions in this region (which create these ions). The CH_5^+ density in the middle of the reactor, between the two electrodes, is of the order of 2×10^{14} m^{-3}. It is interesting to note that all other ionic species are characterized by a similar profile, albeit at somewhat lower densities.[3] A density profile of CH_3 (the main radical) is given in Fig. 5. As can be seen from this figure, the highest

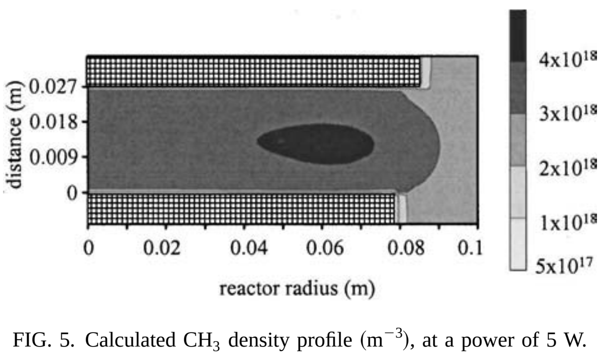

FIG. 5. Calculated CH_3 density profile (m^{-3}), at a power of 5 W.

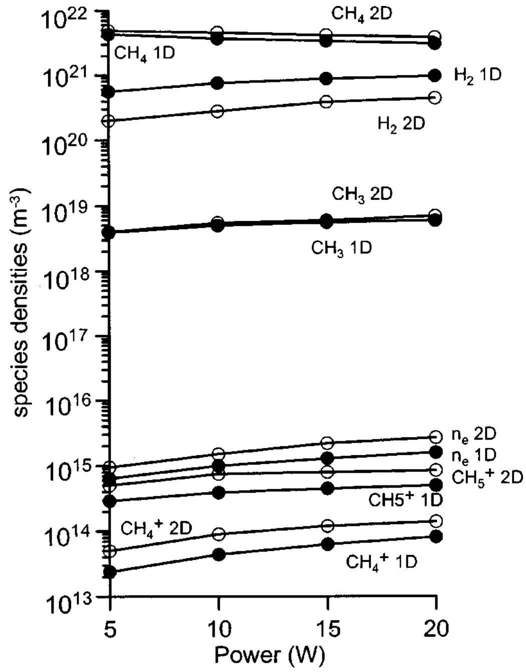

FIG. 6. Calculated densities of the most important plasma species, obtained with the 1D (black circles) and 2D (open circles) model, as a function of power.

CH_3 density (about 4×10^{18} m^{-3}) is again obtained in the radial direction near the side end of the powered electrode, and halfway between the two electrodes in the axial direction. In this region, CH_3 is formed by electron–neutral reactions and neutral–neutral reactions. Outside the region between the two electrodes (i.e., the so-called plasma region), the CH_3 radicals are also present at a relatively high density. This can be explained from the neutral–neutral reactions forming a considerable number of CH_3 radicals. It should be mentioned that analogous density profiles were also obtained for the other radicals present in the model (C_2H_5, H, CH_2, and CH). However, for the CH_2 and CH radicals, the density is only high in the plasma region, and very low outside this region. These species are, indeed, not only formed, but predominantly consumed in the neutral–neutral reactions. The densities of the neutral molecules (CH_4 and others, see Table I) do not show large variations as a function of axial and radical directions (and are therefore not presented here) because the transport of the neutrals is restricted to diffusion in our model. The calculated densities of the neutrals, radicals, and ions are in agreement with the results presented from other 2D models,[8,9] although different reactions and species are considered in the models.

In general, the particle densities for the four simulations obtained with the 1D and 2D fluid models are in relatively good agreement. In Fig. 6, the calculated densities (maximum value) as a function of power are given for the most important plasma species (CH_4, H_2, CH_5^+, CH_4^+, CH_3, and electron density). In the 2D model, the CH_4 density is somewhat higher than in the 1D model, which leads to somewhat lower densities of the other background molecules (H_2, C_2H_6, and others) in the 2D model. Note that the maxima of the species densities in the 1D model are obtained halfway

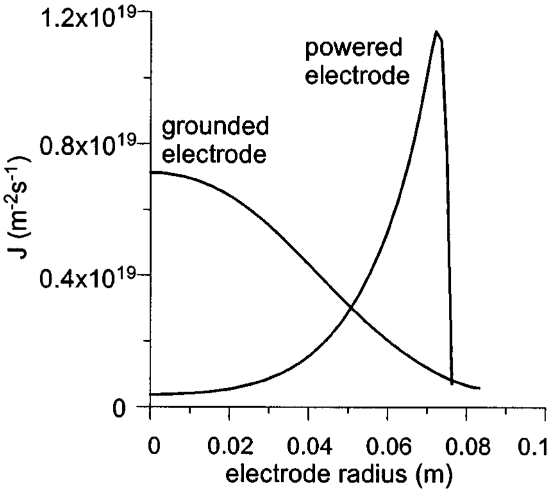

FIG. 7. Calculated time-averaged electron flux towards the powered and grounded electrode, as a function of radial direction, at a power of 5 W.

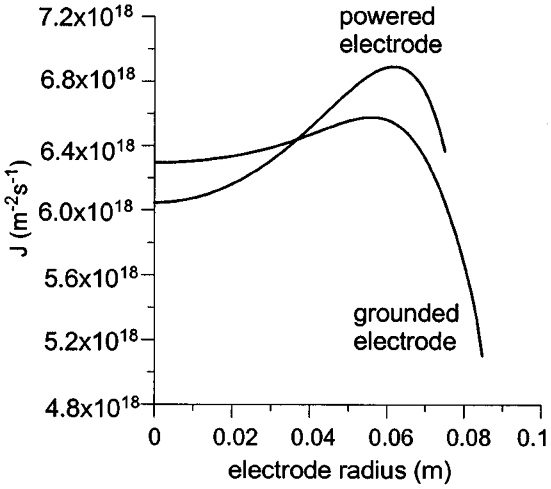

FIG. 9. Calculated CH_3 flux towards the powered and grounded electrode, as a function of radial direction, at a power of 5 W.

between the two electrodes, whereas the maxima of species densities in the 2D model are obtained at a radial position of about 7 cm, between the two electrodes. From this figure, it can be seen that for the four simulations, a relatively good agreement is obtained (as mentioned above, for the 1D model, the calculated species densities were validated with experimental results[3]).

With the 2D model, additional information can be obtained about the species fluxes as a function of radial direction. For the simulation at 5 W, the fluxes of the ions, electrons, and radicals are discussed. Figure 7 presents the calculated time-averaged electron flux towards both electrodes (i.e., powered electrode at the lower side with 7.6 cm radius and grounded electrode at the upper side with a radius of 8.5 cm). It appears that the time-averaged electron flux towards the powered electrode increases from the middle of the electrode (about $10^{18}\ m^{-2}\,s^{-1}$) to the side end of the electrode (about $1.2\times 10^{19}\ m^{-2}\,s^{-1}$). This is logical because the electron density is the highest near the side end of the powered electrode. Due to the larger changes in electric field at the end of the electrode, as a function of time in the rf cycle, more electrons are pushed towards the side end of the powered electrode. The calculated time-averaged electron flux towards the grounded electrode shows an opposite profile. In the middle of the grounded electrode, the time-averaged electron flux has its maximum ($7\times 10^{18}\ m^{-2}\,s^{-1}$), and decreases gradually towards the outer end of the grounded electrode ($10^{18}\ m^{-2}\,s^{-1}$). This electron flux profile can again be explained from the electric field (as a function of rf cycle), which shows some differences as a function of radial direction. However, the difference as a function of radial direction for the time-averaged electron flux towards the grounded electrode is lower than towards the powered electrode. Finally, it is worth mentioning that the electron fluxes towards both electrodes are calculated to be about $3\times 10^{18}\ m^{-2}\,s^{-1}$ in the 1D model, which is of the same order of magnitude as the fluxes obtained with the 2D model (see Fig. 7). However, it should be realized that in the 1D model the fluxes towards both electrodes are equal, because no dc self-bias voltage is formed at the powered electrode.

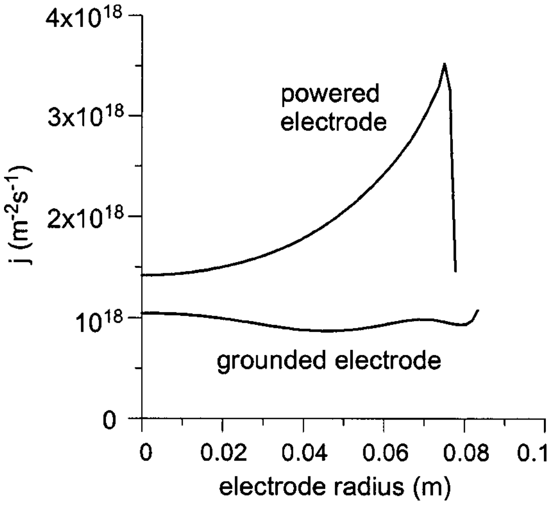

FIG. 8. Calculated time-averaged CH_5^+ ion flux towards the powered and grounded electrode, as a function of radial direction, at a power of 5 W.

The time-averaged ion flux of CH_5^+ (i.e., the main ion in the plasma) towards both electrodes is given in Fig. 8. The time-averaged ion flux towards the powered electrode shows a similar profile as the time-averaged electron flux, and is related to the maximum ion density near the side end of the powered electrode. The CH_5^+ ion flux towards the grounded electrode shows a quite uniform behavior as a function of electrode radius (i.e., about $10^{18}\ m^{-2}\,s^{-1}$). This value of $10^{18}\ m^{-2}\,s^{-1}$ is also calculated with the 1D model for the CH_5^+ ion flux towards both electrodes, hence, the 1D and 2D models yield similar results. Finally, these characteristic ion flux profiles towards both electrodes are also calculated in 2D for all other ionic species.

The calculated fluxes of the main radical, (i.e., CH_3, towards both electrodes are given in Fig. 9. The CH_3 flux towards the grounded electrode is in the order of $6\times 10^{18}\ m^{-2}\,s^{-1}$), and increases slightly as a function of radial direction. It decreases, however, sharply at the side end of the grounded electrode. The calculated CH_3 flux towards

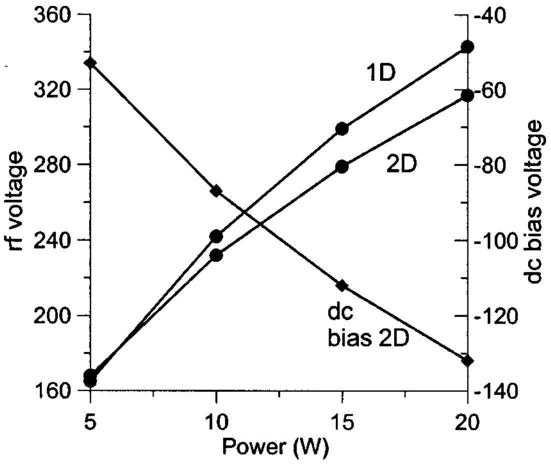

FIG. 10. Comparison of the rf voltage values, as a function of power, as calculated obtained with the 1D and 2D fluid model. The dc self-bias voltage obtained with the 2D fluid model is also given.

the powered electrode shows a similar profile, but here, the difference in flux as a function of radial direction is somewhat larger. The maxima in CH_3 fluxes, at the side end of both electrodes, can again be explained from the fact that the CH_3 density is at its maximum in that region between the electrodes. The CH_3 flux calculated with the 1D model is in the same order (i.e., about $6\times10^{18}\ \mathrm{m}^{-2}\,\mathrm{s}^{-1}$) as the values obtained with the 2D model. For the other radicals, similar flux profiles towards both electrodes have been calculated.

Finally, as mentioned above, the power is one of the inputs in the model. From this power, the voltage at the rf-powered electrode (also called rf voltage), is calculated in both models. Furthermore, the dc bias voltage is also calculated in the 2D model. It should be noted that no dc self-bias can be obtained in the 1D model.

The comparison of the amplitude of the rf voltage values, as calculated with the 1D and 2D fluid models, is shown in Fig. 10, as a function of power. Furthermore, the dc self-bias voltage as calculated with the 2D model, is also plotted for the four simulations. It is clear from Fig. 10 that the rf voltage values obtained with both models are in relatively good agreement for the four power values. This shows that the 1D model produces realistic results. However, the 2D model gives additional information on the dc bias voltage. The rf-voltage values, obtained with both models, show an increase as a function of power. The increase in rf voltage, as a function of power, is also accompanied with a decrease of dc bias voltage in the 2D model.

IV. CONCLUSIONS

A comparison is made between the results of a 1D and 2D fluid model for a methane plasma. Both fluid models are coupled with a simplified Boltzmann model to obtain the electron reaction rate coefficients, as a function of average electron energy. The species densities calculated with both models are in relatively good agreement. The 2D model results reveal that the electrons, ions, and radicals have their maximum density near the side end of the electrodes (in the radial direction), and in the middle between the electrodes (in axial direction). The time-averaged fluxes of the ions and electrons towards the powered electrode show a similar profile. Indeed, these fluxes are characterized by a peak at the end of the electrode. The time averaged electron flux towards the grounded electrode reaches its maximum at the central region of the electrode, whereas the time-averaged ion fluxes to the grounded electrode shows a more or less uniform profile, in radial direction. Finally, the fluxes of the radical species were found to be quite similar towards both electrodes, i.e., increasing slightly as a function of radial direction, and with a sharp drop at the side end of the electrode. The density and flux profiles of the different plasma species can be explained from the changes of the electric field in the radial and axial direction, as a function of rf cycle.

The information concerning the species fluxes towards the electrodes as a function of radial direction is of interest for the uniformity of the deposited layer in PACVD. It is important as an input in a molecular dynamics model that we are currently developing for the simulation of the growth of the layer. Moreover, the 2D model will also be used to investigate the influence of convective flow for the neutrals on the plasma characteristics, which we plan to do in the near future.

ACKNOWLEDGMENTS

The authors acknowledge financial support from the Vlaamse Instelling voor Technologisch Onderzoek (VITO), the Federal Services for Scientific, Technical and Cultural Affairs (DWTC/SSTC) of the Prime Minister's Office through IUAP V, a New Research Initiative of the University of Antwerp, and the Flemish Fund for Scientific Research (FWO).

[1] E. Gogolides, D. Mary, A. Rhaballi, and G. Turban, Jpn. J. Appl. Phys., Part 1 **34**, 261 (1995).
[2] K. Bera, B. Farouk, and Y. H. Lee, J. Electrochem. Soc. **146**, 3264 (1999).
[3] D. Herrebout, A. Bogaerts, M. Yan, R. Gijbels, W. Goedheer, and E. Dekempeneer, J. Appl. Phys. **90**, 570 (2001).
[4] P. M. Meijer, W. J. Goedheer, and J. D. P. Passchier, Phys. Rev. A **45**, 1098 (1992).
[5] G. J. Nienhuis, W. J. Goedheer, E. A. G. Hamers, W. G. J. H. M. van Sark, and J. Bezemer, J. Appl. Phys. **82**, 2060 (1997).
[6] G. J. Nienhuis and W. Goedheer, Plasma Sources Sci. Technol. **8**, 295 (1999).
[7] G. J. Nienhuis, Ph.D. thesis, Utrecht University, 1998.
[8] K. Bera, J. W. Yi, B. Farouk, and Y. H. Lee, IEEE Trans. Plasma Sci. **27**, 5 (1999).
[9] K. Bera, B. Farouk, and Y. H. Lee, Plasma Sources Sci. Technol. **10**, 211 (2001).
[10] K. Bera, B. Farouk, and Y. H. Lee, Plasma Sources Sci. Technol. **8**, 412 (1999).
[11] K. Nagayama, B. Farouk, and Y. H. Lee, IEEE Trans. Plasma Sci. **26**, 125 (1998).
[12] E. Gogolides and H. Sawin, J. Appl. Phys. **72**, 3971 (1992).
[13] J. D. P. Passchier, Ph.D. thesis, Utrecht University, 1994.
[14] J. D. P. Passchier and W. J. Goedheer, J. Appl. Phys. **74**, 3744 (1993).
[15] D. L. Sharfetter and H. K. Gummel, IEEE Trans. Electron Devices **ED-16**, 64 (1969).